

Article

# Cooperative Decay of $N$ Atoms in a Ring Configuration

Nicola Piovella 

Dipartimento di Fisica “Aldo Pontremoli”, Università degli Studi di Milano, Via Celoria 16, I-20133 Milano, Italy; nicola.piovella@unimi.it

**Abstract:** We provide an analytic expression of the spectrum of the cooperative decay rate of  $N$  two-level atoms regularly distributed on a ring in the single-excitation configuration. The results are obtained first for the scalar model and then extended to the vectorial light model, assuming all the dipoles are aligned.

**Keywords:** superradiance; subradiance; cooperative emission

## 1. Introduction

In this paper, we study the cooperative emission of an array of identical two-level atoms, organized in a circular ring of radius  $\rho$ . This study is part of the general subject of cooperative spontaneous emission by  $N$  excited two-level atoms, extensively studied since the seminal work by Dicke in 1954 [1] and Lehmberg in 1970 [2]. It includes the well-known effect of superradiance, i.e., enhanced spontaneous emission due to constructive interference between the emitters [3,4], and subradiance, i.e., inhibited emission due to destructive interference between the emitters, which is more elusive and difficult to observe [5–9]. Subradiance has seen a large increase in interest in the last few years, as it offers the opportunity of storing photons in emitter ensembles for times longer than the single emitter lifetime [10–17]. In particular, superradiance and subradiance have been studied in the single-excitation configuration, belonging to the regime of linear optics. In disordered systems, the cooperative decay must be studied numerically, usually by solving the dynamics of an initially excited ensemble [18,19]. A more appealing situation is when the atoms form ordered arrays, where cooperativity may be enhanced. For instance, infinite and finite linear chains of two-level atoms are considered in ref. [14,15,20,21]. Subradiance has been experimentally observed also in a bidimensional lattice [22] or in an ensemble of atoms coupled to the guided mode of an optical nanofiber [23].

Having recently studied the finite chain of atoms [21], we are interested here in studying the decay rates when the atoms form a closed configuration since it is expected to lead to a stronger suppression of the excitation. The cooperative single-quantum excitation of a closed-ring chain was studied in the past in ref. [24] and more recently in [14,15,20,25]. Starting from the effective non-Hermitian Hamiltonian, which includes an imaginary part describing the cooperative spontaneous decay and a real part describing the cooperative energy shift [2,26], we focus on the cooperative decay only, calculating analytically the spectrum of the decay rates. The analysis is carried out by initially assuming the scalar model of light and neglecting the vectorial nature of the dipoles. The scalar model is particularly attractive because, since the polarization direction does not play any role, it is able to catch the main features of cooperativity just considering the relative phases of the emitters. Then, we extend the results to the vectorial light model for a set of  $N$  equally oriented dipoles.



Academic Editors: Eugene T. Kennedy and Mark Edwards

Received: 19 December 2024

Revised: 10 January 2025

Accepted: 14 January 2025

Published: 16 January 2025

**Citation:** Piovella, N. Cooperative Decay of  $N$  Atoms in a Ring Configuration. *Atoms* **2025**, *13*, 8. <https://doi.org/10.3390/atoms13010008>

**Copyright:** © 2025 by the author. Licensee MDPI, Basel, Switzerland. This article is an open access article distributed under the terms and conditions of the Creative Commons Attribution (CC BY) license (<https://creativecommons.org/licenses/by/4.0/>).

## 2. Scalar Model

We consider  $N$  identical two-level atoms with transition frequency  $\omega_0 = ck_0$ , linewidth  $\Gamma$ , and dipole  $\mu$ . The atoms are prepared in a single-excitation state;  $|g_j\rangle$  and  $|e_j\rangle$  are the ground and excited states, respectively, of the  $j$ -th atom,  $j = 1, \dots, N$ , which is placed at position  $\mathbf{r}_j$ . We consider here the single-excitation effective Hamiltonian in the scalar approximation, whereas the exact vectorial model will be considered later. If we assume that only one photon is present, when tracing over the radiation degrees of freedom, the dynamics of the atomic system can be described by the non-Hermitian Hamiltonian [19,27]

$$\hat{H} = -i\frac{\hbar}{2} \sum_{j,m} G_{jm} \hat{\sigma}_j^\dagger \hat{\sigma}_m, \tag{1}$$

where  $\hat{\sigma}_j = |g_j\rangle\langle e_j|$  and  $\hat{\sigma}_j^\dagger = |e_j\rangle\langle g_j|$  are the lowering and raising operators,  $G_{jm}$  is the scalar Green function,

$$G_{jm} = \begin{cases} \Gamma_{jm} - i\Omega_{jm} & \text{if } j \neq m, \\ \Gamma & \text{if } j = m, \end{cases} \tag{2}$$

and

$$\Gamma_{jm} = \Gamma \frac{\sin(k_0 r_{jm})}{k_0 r_{jm}}, \quad \Omega_{jm} = \Gamma \frac{\cos(k_0 r_{jm})}{k_0 r_{jm}}, \tag{3}$$

where  $r_{jm} = |\mathbf{r}_j - \mathbf{r}_m|$ .  $\hat{H}$  contains both real and imaginary parts, which takes into account that the excitation is not conserved since it can leave the system by emission. We focus our attention on the decay term  $\Gamma_{jm}$ .

We consider  $N$  atoms on a ring of radius  $\rho$  and angles  $\phi_j = (2\pi/N)(j - 1)$ , with  $j = 1, \dots, N$  (see Figure 1).

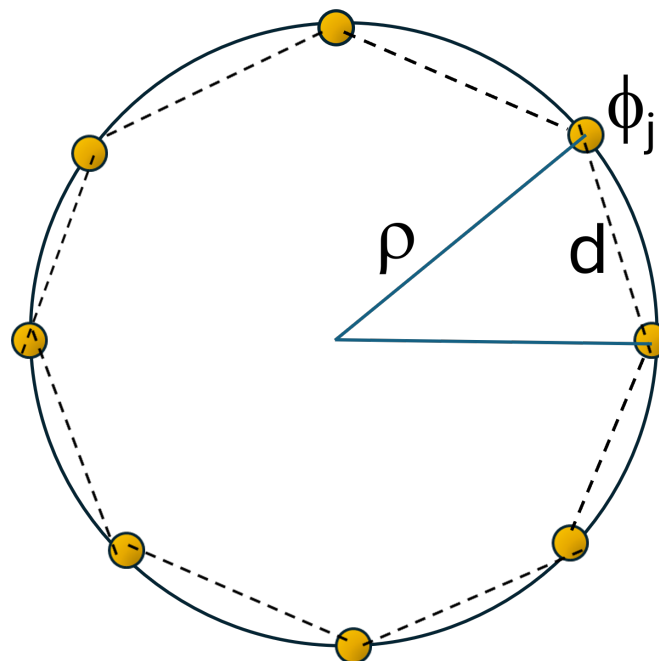


**Figure 1.** Scheme of the system: a ring with interparticle distance  $d$ , radius  $\rho$ , and angular position given by  $\phi_j = 2\pi(j - 1)/N$ .

We write

$$\Gamma_{jm} = \Gamma \frac{\sin(k_0 r_{jm})}{k_0 r_{jm}} = \frac{\Gamma}{2} \int_{-1}^1 e^{i(k_0 r_{jm})t} dt \tag{4}$$

where  $k_0 r_{jm} = 2k_0 \rho \sin(\phi_{jm}/2)$  and  $\phi_{jm} = \phi_j - \phi_m$ . Then, we expand the exponential

$$e^{2iat \sin(\phi_{jm}/2)} = J_0(2at) + 2 \sum_{n=1}^{\infty} J_{2n}(2at) \cos(n\phi_{jm}) + 2i \sum_{n=1}^{\infty} J_{2n+1}(2at) \cos[(2n+1)\phi_{jm}/2]$$

where  $a = k_0 \rho$ . The last term is odd in  $t$ , so it can be dropped from the integral in Equation (4), obtaining

$$\Gamma_{jm} = \Gamma \sum_{n=-\infty}^{+\infty} c_n(a) e^{in(\phi_j - \phi_m)} \tag{5}$$

where

$$c_n(a) = \int_0^1 J_{2n}(2at) dt = \frac{a^{2n}}{\Gamma(2+2n)} {}_1F_2[1/2+n; 3/2+n, 1+2n; -a^2] \tag{6}$$

where  ${}_1F_2[\alpha; \beta_1, \beta_2; z]$  is the Hypergeometric PFQ function and  $\Gamma(n)$  is the gamma function. Notice that  $c_n(a) = c_{-n}(a)$  and

$$\sum_{n=-\infty}^{+\infty} c_n(a) = 1 \tag{7}$$

so that  $\Gamma_{jj} = \Gamma$ . We define the spectrum of the decay rates as [25]

$$\Gamma_k = \frac{1}{N} \sum_{j,m=1}^N e^{ik\phi_{jm}} \Gamma_{jm} \tag{8}$$

where  $k = -N/2, \dots, N/2$  is discrete (let us suppose  $N$  is even). Since by Equation (5) the sum on  $j$  and  $m$  factorizes, we obtain

$$\Gamma_k = \frac{\Gamma}{N} \sum_{n=-\infty}^{+\infty} c_n(a) |F_{k+n}|^2 \tag{9}$$

where

$$|F_k|^2 = \left| \sum_{j=1}^N e^{ik(2\pi/N)(j-1)} \right|^2 = \frac{\sin^2(k\pi)}{\sin^2(k\pi/N)} = N^2 \sum_{m=-\infty}^{+\infty} \delta_{k,mN} \tag{10}$$

and

$$\Gamma_k = \Gamma N \sum_{m=-\infty}^{+\infty} c_{k-mN}(a). \tag{11}$$

The advantage of this expression is that is valid for an arbitrarily large number of atoms  $N$ . Furthermore, the spectrum is symmetric, with  $\Gamma_{-k} = \Gamma_k$ . Equation (11) is the main result of the paper.

### Analysis

It results that  $c_n(a) \approx 0$  for  $|n| > a$ ; for  $a \rightarrow 0$ ,  $c_n(a) = \delta_{n,0}$ , whereas for  $a \gg 1$ ,  $c_n(a) \sim 1/(2a)$  for  $|n| < a$  (see the example of Figure 2 for  $a = 50$ ).

Hence, in the limit  $a \rightarrow 0$ ,  $\Gamma_k = \Gamma N \delta_{k,0}$ : the spectrum is composed by a single superradiant component  $k = 0$  and the remaining subradiant components with  $k \neq 0$  (Dicke limit). If  $a < N/2$ ,  $\Gamma_k \approx 0$  for  $|k| > a$  (subradiance). Instead, assuming  $a \gg N/2$ , the sum of Equation (11) spans from  $-m_{\max}$  to  $m_{\max}$ , where  $m_{\max}$  is determined by the condition  $m_{\max} N - k \sim a$ . Hence,

$$m_{\max} \sim \frac{a}{N} + \frac{k}{N} \sim \frac{a}{N} \tag{12}$$

since  $|k| < N/2$  and  $a \gg N$ . Then, Equation (11) gives, in the limit  $a \gg N/2$ ,

$$\Gamma_k \sim \Gamma N \sum_{m=-m_{\max}}^{m_{\max}} c_{k-mN}(a) \sim \Gamma N \frac{1}{2a} \frac{2a}{N} \sim \Gamma. \tag{13}$$

As expected, when  $a/N$  becomes very large, the distance  $d$  between adjacent atoms becomes much larger than the wavelength  $\lambda_0$ , and cooperativity disappears. Ref. [14] investigated numerically a ring distribution of  $N$  atoms with fixed atom–atom separation  $d$ . In our case, the spectrum of the decay rate is a function of radius  $\rho$  and of the number of atoms  $N$ . The distance  $d$  between adjacent atoms is  $d = 2\rho \sin(\pi/N) \approx 2\pi\rho/N$ , where the last expression is valid for large  $N$ . The previous necessary condition for subradiance,  $k_0\rho < N/2$ , implies  $d/\lambda_0 < 0.5$ . As discussed before, the sum in Equation (11) spans from  $-m_{\max}$  to  $+m_{\max}$ , where  $m_{\max}$  is determined by  $m_{\max}N - k \sim k_0\rho \sim (d/\lambda_0)N$  so that  $m_{\max} \sim (k/N) + (d/\lambda_0)$ . Taking the most subradiant value  $k = N/2$  (since subradiance occurs for  $(d/\lambda_0)N < k < N/2$ ), then  $m_{\max} \sim (d/\lambda_0) + 0.5 < 1$ , and the only term surviving in the sum of Equation (11) is  $m = 0$ :

$$\Gamma_{N/2} \sim \Gamma N c_{N/2}(dN/\lambda_0) \tag{14}$$

For  $N \gg 1$ ,

$$\Gamma_{N/2} \sim \Gamma J_N(2dN/\lambda_0) \sim \frac{1}{\sqrt{2\pi N}} (ed/\lambda_0)^N, \tag{15}$$

where  $J_n(x)$  is the Bessel function of order  $n$ , and the last expression is valid when  $ed/\lambda_0 < 1$ . In conclusion, the spontaneous emission is exponentially suppressed, as seen in ref. [14], if we increase  $N$ , keeping the distance between adjacent atoms constant, i.e., increasing the radius  $\rho$  proportionally to  $N$ . On the contrary, in the continuous limit, we tend to let  $N \rightarrow \infty$  and  $d/\lambda_0 \rightarrow 0$  such that  $k_0\rho$  remains finite. Then, in the sum of Equation (11), there remains only the term  $m = 0$ , and

$$\Gamma_k^{\text{cont}} \sim \Gamma N c_k(k_0\rho) \tag{16}$$

Subradiance occurs for  $k_0\rho < |k| < N/2$ , whereas superradiance occurs for  $|k| < k_0\rho$ . When  $k_0\rho \rightarrow 0$ , then  $\Gamma_k^{\text{cont}} \sim \Gamma N \delta_{k,0}$ , whereas when  $k_0\rho \gg 1$ , then  $\Gamma_k^{\text{cont}} \sim \Gamma N / (2k_0\rho)$  when  $|k| < k_0\rho$ .

In Figure 3, we plot the decay rate for different values of  $k = 0, 1, 2, 4$  for  $N = 10$  as a function of  $\lambda_0/d$ . We see that as  $\lambda_0/d \rightarrow 0$ ,  $\Gamma_k \approx \Gamma N / 2a \sim (\Gamma/2)(\lambda_0/d)$  (dashed line), whereas for  $\lambda_0/d \rightarrow \infty$ , the emitters are so close that the range of interaction is effectively infinite, yielding a single superradiant mode decaying at rate  $N\Gamma$  and  $N - 1$  perfectly subradiant modes. This may be explained since  $\Gamma_k \approx 0$  for  $k > a$ ; since  $a \approx N(d/\lambda_0)$ , when  $\lambda_0/d \rightarrow \infty$ ,  $a \rightarrow 0$  and the mode  $k = 0$  decays superradiantly as  $N\Gamma$ , whereas the other modes with  $k > 0$  are dark. Conversely, when  $\lambda_0/d \ll 1$ ,  $a \gg 1$  and  $\Gamma_k \sim N\Gamma / (2a) \sim \Gamma(\lambda_0/2d)$ . The results are in agreement with those presented in Ref. [25].

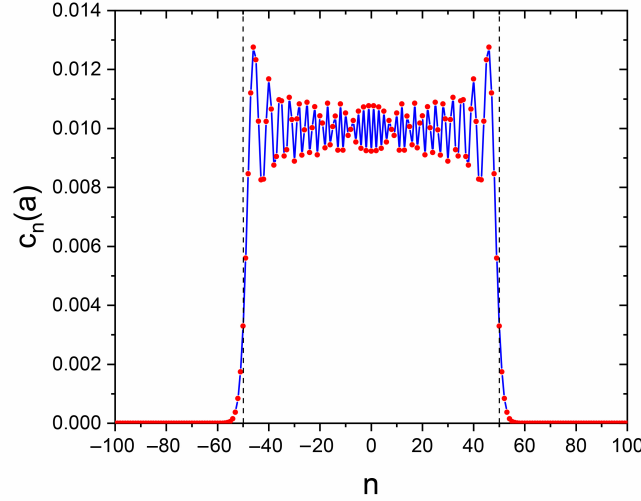


**Figure 2.**  $c_n(a)$  vs.  $n$  for  $a = 50$ . Vertical dashed lines are for  $n = \pm a$ .

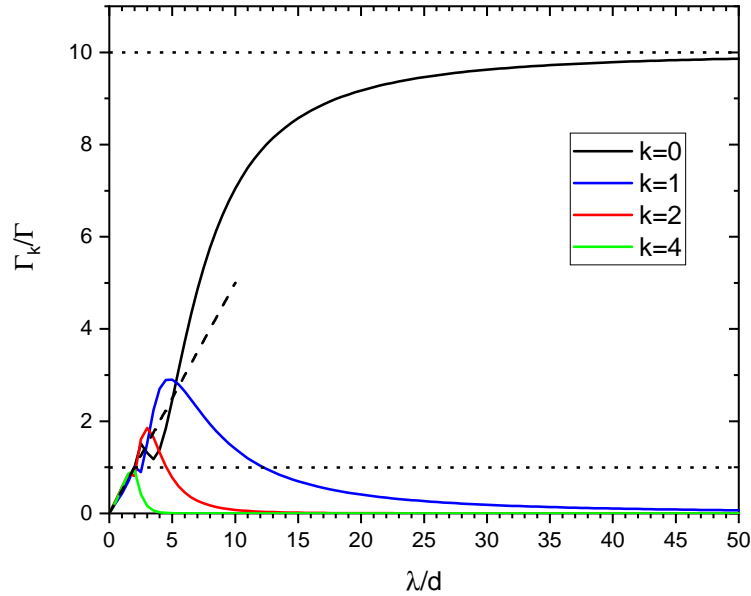


**Figure 3.**  $\Gamma_k/\Gamma$  vs.  $\lambda_0/d$  for  $N = 10$  and  $k = 0, 1, 2, 4$ . In the Dicke limit,  $\lambda_0/d \rightarrow \infty$ , only the superradiant  $k = 0$  with a decay rate  $N\Gamma$  is present, and  $N - 1$  modes are completely subradiant. In the limit  $\lambda_0/d \rightarrow 0$ , all the modes decay with the rate  $\Gamma_k/\Gamma = \lambda_0/2d$  (dashed line).

### 3. Vectorial Model

We now extend the previous expressions to the vectorial model, taking into account the polarization of the electromagnetic field. The non-Hermitian Hamiltonian is now

$$\hat{H} = -i\frac{\hbar}{2} \sum_{\alpha,\beta} \sum_{j,j'} G_{\alpha,\beta}(\mathbf{r}_j - \mathbf{r}_{j'}) \hat{\sigma}_{j,\alpha}^\dagger \hat{\sigma}_{j',\beta}. \tag{17}$$

where  $\alpha, \beta = (x, y, z)$ . Here  $\hat{\sigma}_{j,x} = (\hat{\sigma}_j^{m_J=1} + \hat{\sigma}_j^{m_J=-1})/2$ ,  $\hat{\sigma}_{j,y} = (\hat{\sigma}_j^{m_J=1} - \hat{\sigma}_j^{m_J=-1})/2i$  and  $\hat{\sigma}_{j,z} = \hat{\sigma}_j^{m_J=0}$ , where  $\hat{\sigma}_j^{m_J} = |g_j\rangle\langle e_j^{m_J}|$  is the lowering operator between the ground state  $|g_j\rangle$  and the three excited states  $|e_j^{m_J}\rangle$  of the  $j$ th atom with quantum numbers  $J = 1$  and  $m_J = (-1, 0, 1)$ . The vectorial Green function in Equation (17) is

$$G_{\alpha,\beta}(\mathbf{r}) = \frac{3\Gamma}{2} \frac{e^{ik_0r}}{ik_0r} \left[ \delta_{\alpha,\beta} - \hat{n}_\alpha \hat{n}_\beta + (\delta_{\alpha,\beta} - 3\hat{n}_\alpha \hat{n}_\beta) \left( \frac{i}{k_0r} - \frac{1}{k_0^2 r^2} \right) \right] \tag{18}$$

with  $r = |\mathbf{r}|$  and  $\hat{n}_\alpha$  being the components of the unit vector  $\hat{\mathbf{n}} = \mathbf{r}/r$ . We consider a ring with  $r_{jm} = 2\rho \sin(\phi_{jm}/2)$  and all the dipoles aligned with an angle  $\delta$  with respect to ring's plane so that  $\hat{n}_\alpha = \hat{n}_\beta = \cos \delta$  and

$$G^{(\delta)}(r_{jm}) = \frac{3\Gamma}{2} \frac{e^{ik_0 r_{jm}}}{ik_0 r_{jm}} \left[ \sin^2 \delta + (1 - 3 \cos^2 \delta) \left( \frac{i}{k_0 r_{jm}} - \frac{1}{k_0^2 r_{jm}^2} \right) \right]. \tag{19}$$

The decay rate for the vectorial model is given by the real part of  $G^{(\delta)}(r_{jm})$ ,

$$\Gamma^{(\delta)}(r_{jm}) = \frac{3\Gamma}{2} \left[ \sin^2 \delta j_0(k_0 r_{jm}) + (3 \cos^2 \delta - 1) \frac{j_1(k_0 r_{jm})}{k_0 r_{jm}} \right] \tag{20}$$

where  $j_0(x) = \sin x/x$  and  $j_1(x) = \sin x/x^2 - \cos x/x$  are the spherical Bessel functions of the orders  $n = 0$  and  $n = 1$ . By using the identities

$$\begin{aligned} j_0(x) &= \frac{1}{2} \int_{-1}^1 e^{ixt} dt \\ j_0(x) - 2 \frac{j_1(x)}{x} &= \frac{1}{2} \int_{-1}^1 t^2 e^{ixt} dt, \end{aligned}$$

we can write

$$\begin{aligned} \Gamma^{(\delta)}(r_{jm}) &= \frac{3\Gamma}{8} \left\{ (1 + \cos^2 \delta) \int_{-1}^1 e^{i(k_0 r_{jm})t} dt + (1 - 3 \cos^2 \delta) \int_{-1}^1 t^2 e^{i(k_0 r_{jm})t} dt \right\} \\ &= \frac{3\Gamma}{4} \sum_{n=-\infty}^{\infty} \left\{ (1 + \cos^2 \delta) c_n(a) + (1 - 3 \cos^2 \delta) d_n(a) \right\} e^{in(\phi_j - \phi_m)} \end{aligned} \tag{21}$$

where  $a = k_0 \rho$  and

$$d_n(a) = \int_0^1 t^2 J_{2n}(2at) dt = \frac{a^{2n}}{2} \frac{\Gamma(3/2 + n)}{\Gamma(1 + 2n)\Gamma(5/2 + n)} {}_1F_2[3/2 + n; 5/2 + n, 1 + 2n; -a^2] \tag{22}$$

As before, the spectrum is

$$\Gamma_k^{(\delta)} = \frac{1}{N} \sum_{j,m=1}^N e^{ik\phi_{jm}} \Gamma_{jm}^{(\delta)} \tag{23}$$

where  $k = -N/2, \dots, N/2$  is discrete (let suppose  $N$  even). Then,

$$\Gamma_k^{(\delta)} = \frac{3\Gamma}{4N} \sum_{n=-\infty}^{+\infty} \left\{ (1 + \cos^2 \delta) c_n(a) + (1 - 3 \cos^2 \delta) d_n(a) \right\} |F_{k+n}|^2 \tag{24}$$

and

$$\Gamma_k^{(\delta)} = \frac{3\Gamma N}{4} \sum_{m=-\infty}^{+\infty} \left\{ (1 + \cos^2 \delta) c_{k-mN}(a) + (1 - 3 \cos^2 \delta) d_{k-mN}(a) \right\} \tag{25}$$

It results again that  $d_n(a) \approx 0$  for  $|n| > a$ ; for  $a \rightarrow 0$ ,  $d_n(a) = (1/3)\delta_{n,0}$ , whereas for  $a \gg 1$ ,  $d_n(a) \sim 1/(2a^3)(n^2 - 1/4)$  for  $|n| < a$  (see the example of Figure 4 for  $a = 50$ ).

Hence, in the limit  $a \rightarrow 0$ ,  $\Gamma_k^{(\delta)} = \Gamma N$ , whereas for  $a \gg 1$  and  $|k| < a$ ,

$$\Gamma_k^{(\delta)} = \frac{3\Gamma N}{8a} \left\{ 1 + \cos^2 \delta + \frac{1}{a^2} (1 - 3 \cos^2 \delta) (k^2 - 1/4) \right\} \tag{26}$$

As for the scalar model, we plot in Figure 5 the decay rate  $\Gamma_k^{(\delta)}$  (in units of  $\Gamma$ ) for  $N = 10$  and for different values of  $k = 0, 1, 2, 4$  as a function of  $\lambda_0/d$  for  $\delta = 0$ . The

curves are similar to those of the scalar model. The only difference is that as  $\lambda_0/d \rightarrow 0$ ,  $\Gamma_k^{(\delta)} \approx (3\Gamma/4)(\lambda_0/d)$  (dashed line in Figure 5).

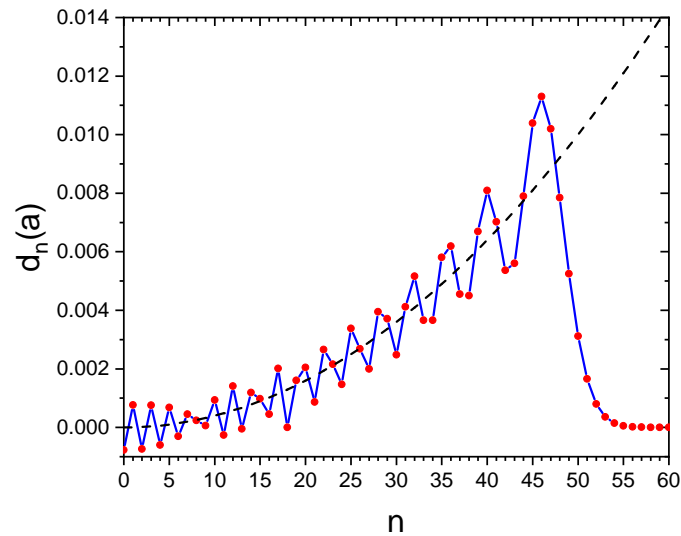


**Figure 4.**  $d_n(a)$  vs.  $n$  for  $a = 50$ . The red dots are the exact solution of Equation (22) and the dashed line is the approximated solution  $d_n(a) \sim 1/(2a^3)(n^2 - 1/4)$ .

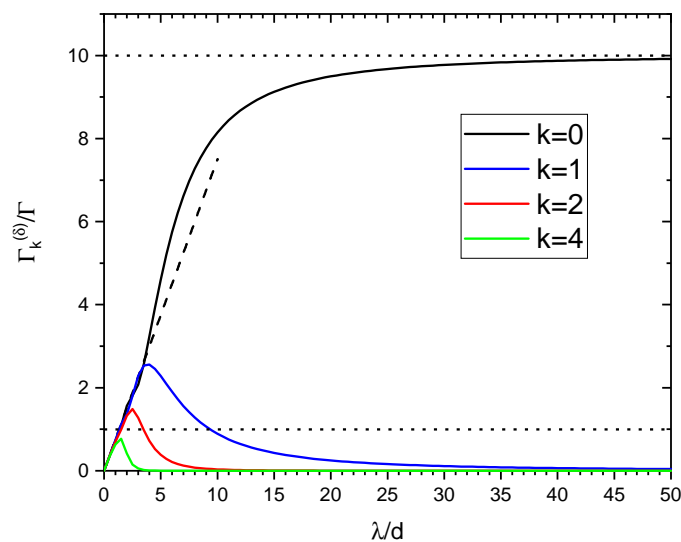


**Figure 5.**  $\Gamma_k^{(\delta)}/\Gamma$  vs.  $\lambda_0/d$  for  $N = 10$  and  $k = 0, 1, 2, 4$ , for  $\delta = 0$ . In the Dicke limit,  $\lambda_0/d \rightarrow \infty$ , only the superradiant  $k = 0$  with a decay rate  $N\Gamma$  is present, and  $N - 1$  modes are completely subradiant. In the limit  $\lambda_0/d \rightarrow 0$ , all the modes decay with the rate  $\Gamma_k^{(\delta)}/\Gamma = (3/4)(\lambda_0/d)$  (dashed line).

### 4. Conclusions

In conclusion, we have presented an analytical expression for the discrete spectrum  $\Gamma_k$  of the decay rates of  $N$  atoms regularly distributed on a ring in the single-excitation configuration, both in the scalar and in the vectorial model. The results are in agreements with those presented in Refs. [14,25], where the rates are calculated numerically as the imaginary part of the eigenvalues of the effective Hamiltonian. The analytical expression shows that the decay rates are proportional to  $N$  times a function of the parameter  $a = k_0\rho$ , where  $\rho$  is the ring’s radius. The modes with  $|k| > a$  are dark, with almost zero decay rates, whereas the modes with  $|k| < a$  are superradiant, with  $\Gamma_k \sim N\Gamma/(2a)$  for large values of  $a$ . Keeping fixed the distance  $d \sim 2\pi\rho/N$  between adjacent atoms on the ring, the most subradiant modes decay exponentially with  $N$  when  $d/\lambda_0 < 0.5$  as seen in Ref. [14]. Is it

interesting to note that in the ring configuration, the subradiant spectrum depends on the parameter  $a$  and not on the atomic number  $N$ , as it occurs, for instance, in a finite linear chain [21].

These analytical results may be important for the future implementation in experimental setups. While ring configurations are not so easy to implement using individual atoms in optical traps, closely related ring-shaped structures of dipoles appear naturally in biological light harvesting complexes [28] or can be set up using quantum dot micro-arrays [29]. Alternatively, one could study such structures in tweezer arrays [30]. As a potential utility of the present results, it has been shown that subradiance may reduce errors for applications such as quantum memories, enabling more efficient quantum information processing and quantum communication protocols [31], or may greatly extend the excited-state lifetimes in optical-lattice clocks [32].

**Funding:** This research received no external funding.

**Data Availability Statement:** Data are contained within the article.

**Conflicts of Interest:** The author declares no conflicts of interest.

## References

1. Dicke, R.H. Coherence in spontaneous radiation processes. *Phys. Rev.* **1954**, *93*, 99. [[CrossRef](#)]
2. Lehmburg, R.H. Radiation from an N-Atom system, I. General formalism. *Phys. Rev. A* **1970**, *2*, 883. [[CrossRef](#)]
3. Gross, M.; Haroche, S. Superradiance: An Essay on the Theory of Collective Spontaneous Emission. *Phys. Rep.* **1982**, *93*, 301. [[CrossRef](#)]
4. Bonifacio, R.; Schwendimann, P.; Haake, F. Quantum Statistical Theory of Superradiance I. *Phys. Rev. A* **1971**, *4*, 302. [[CrossRef](#)]
5. Crubellier, A.; Liberman, S.; Pavolini, D.; Pillet, P. Superradiance and subradiance. I. Interatomic interference and symmetry properties in three-level systems. *J. Phys. B: Atom. Mol. Phys.* **1985**, *18*, 3811. [[CrossRef](#)]
6. Bienaimé, T.; Piovella, N.; Kaiser, R. Controlled Dicke subradiance from a large cloud of two-level systems. *Phys. Rev. Lett.* **2012**, *108*, 123602. [[CrossRef](#)]
7. Guerin, W.; Araùjo, M.O.; Kaiser, R. Subradiance in a Large Cloud of Cold Atoms. *Phys. Rev. Lett.* **2016**, *116*, 083601. [[CrossRef](#)]
8. Ferioli, G.; Glicenstein, A.; Henriët, L.; Ferrier-Barbut, I.; Browaeys, A. Storage and Release of Subradiant Excitations in a Dense Atomic Cloud. *Phys. Rev. X* **2021**, *11*, 021031. [[CrossRef](#)]
9. Cipris, A.; Moreira, N.A.; do Espirito Santo, T.S.; Weiss, P.; Villas-Boas, C.J.; Kaiser, R.; Guerin, W.; Bachelard, R. Subradiance with Saturated Atoms: Population Enhancement of the Long-Lived States. *Phys. Rev. Lett.* **2021**, *126*, 103604. [[CrossRef](#)]
10. Scully, M.O. Single photon subradiance: Quantum control of spontaneous emission and ultrafast readout. *Phys. Rev. Lett.* **2015**, *115*, 243602. [[CrossRef](#)] [[PubMed](#)]
11. Jen, H.H.; Chang, M.S.; Chen, Y.C. Cooperative single-photon subradiant states. *Phys. Rev. A* **2016**, *94*, 013803. [[CrossRef](#)]
12. Facchinetti, G.; Jenkins, S.D.; Ruostekoski, J. Storing light with subradiant correlations in arrays of atoms. *Phys. Rev. Lett.* **2016**, *117*, 243601. [[CrossRef](#)] [[PubMed](#)]
13. Bettles, R.J.; Gardiner, S.A.; Adams, C.S. Cooperative eigenmodes and scattering in one-dimensional atomic arrays. *Phys. Rev. A* **2016**, *94*, 043844. [[CrossRef](#)]
14. Asenjo-Garcia, A.; Moreno-Cardoner, M.; Albrecht, A.; Kimble, H.J.; Chang, D.E. Exponential improvement in photon storage fidelities using subradiance and “selective radiance” in atomic arrays. *Phys. Rev. X* **2017**, *7*, 031024. [[CrossRef](#)]
15. Needham, J.A.; Lesanovsky, I.; Olmos, B. Subradiance-protected excitation transport. *New J. Phys.* **2019**, *21*, 073061. [[CrossRef](#)]
16. Reitz, M.; Sommer, C.; Genes, C. Cooperative Quantum Phenomena in Light-Matter Platforms. *Prx Quantum* **2022**, *3*, 010201. [[CrossRef](#)]
17. Stiesdal, N.; Busche, H.; Kumlin, J.; Kleinbeck, K.; Büchler, H.P.; Hofferberth, S. Observation of collective decay dynamics of a single Rydberg superatom. *Phys. Rev. Res.* **2020**, *2*, 043339. [[CrossRef](#)]
18. Scully, M.O.; Fry, E.; Ooi, C.H.R.; Wodkiewicz, K. Directed Spontaneous Emission from an Extended Ensemble of N Atoms: Timing Is Everything. *Phys. Rev. Lett.* **2006**, *96*, 010501. [[CrossRef](#)]
19. Bienaimé, T.; Bachelard, R.; Piovella, N.; Kaiser, R. Cooperativity in light scattering by cold atoms. *Fortschritte Physik* **2013**, *61*, 377. [[CrossRef](#)]
20. Cech, M.; Lesanovsky, I.; Olmos, B. Dispersionless subradiant photon storage in one-dimensional emitter chains. *Phys. Rev. A* **2023**, *108*, L051702. [[CrossRef](#)]

21. Piovela, N. Cooperative Decay of an Ensemble of Atoms in a One-Dimensional Chain with a Single Excitation. *Atoms* **2024**, *12*, 43. [[CrossRef](#)]
22. Rui, J.; Wei, D.; Rubio-Abadal, A.; Hollerith, S.; Zeiher, J.; Stamper-Kurn, D.M.; Christian Gross, C.; Bloch, I. A subradiant optical mirror formed by a single structured atomic layer. *Nature* **2020**, *583*, 369. [[CrossRef](#)]
23. Pennetta, R.; Lechner, D.; Blaha, M.; Rauschenbeutel, A.; Schneeweiss, P.; Volz, J. Observation of Coherent Coupling between Super- and Subradiant States of an Ensemble of Cold Atoms Collectively Coupled to a Single Propagating Optical Mode. *Phys. Rev. Lett.* **2022**, *128*, 203601. [[CrossRef](#)] [[PubMed](#)]
24. Freedhoff, H.S. Cooperative single-quantum excitations of a closed-ring polymer chain. *J. Chem. Phys.* **1986**, *85*, 6110. [[CrossRef](#)] [[PubMed](#)]
25. Coreno-Cardoner, M.; Plankensteiner, D.; Ostermann, L.; Chang, D.E.; Ritsch, H. Subradiant-enhanced excitation transfer between dipole-coupled nanorings of quantum emitters. *Phys. Rev. A* **2019**, *100*, 023806. [[CrossRef](#)]
26. Friedberg, R.; Hartman, S.R.; Manassah, J.T. Frequency shifts in emission and absorption by resonant systems of two-level atoms. *Phys. Rep.* **1973**, *7*, 101. [[CrossRef](#)]
27. Akkermans, E.; Gero, A.; Kaiser, R. Photon localization and Dicke superradiance in atomic gases. *Phys. Rev. Lett.* **2008**, *101*, 103602. [[CrossRef](#)]
28. Law, C.J.; Roszak, A.W.; Southall, J.; Gardiner, A.T.; Isaacs, N.W.; Cogdell, R.J. The structure and function of bacterial light-harvesting complexes (review). *Mol. Membr. Biol.* **2004**, *21*, 183. [[CrossRef](#)]
29. Richner, P.; Eghlidi, H.; Kress, S.J.; Schmid, M.; Norris, D.J.; Poulidakos, D. Printable nanoscopic metamaterial absorbers and images with diffraction-limited resolution. *ACS Appl. Mater. Interfaces* **2016**, *8*, 11690. [[CrossRef](#)] [[PubMed](#)]
30. Barredo, D.; de Léséleuc, S.; Lienhard, V.; Lahaye, T.; Browaeys, A. An atom-by-atom assembler of defect-free arbitrary two-dimensional atomic arrays. *Science* **2016**, *354*, 1021. [[CrossRef](#)] [[PubMed](#)]
31. Manzoni, M.T.; Moreno-Cardoner, M.; Asenjo-Garcia, A.; Porto, J.V.; Gorshkov, A.V.; Chang, D.E. Optimization of photon storage fidelity in ordered atomic arrays. *New J. Phys.* **2018**, *20*, 083048. [[CrossRef](#)]
32. Henriot, L.; Douglas, J.S.; Chang, D.E.; Albrecht, A. Critical open-system dynamics in a one-dimensional optical-lattice clock. *Phys. Rev. A* **2019**, *99*, 023802. [[CrossRef](#)] [[PubMed](#)]

**Disclaimer/Publisher's Note:** The statements, opinions and data contained in all publications are solely those of the individual author(s) and contributor(s) and not of MDPI and/or the editor(s). MDPI and/or the editor(s) disclaim responsibility for any injury to people or property resulting from any ideas, methods, instructions or products referred to in the content.